J. Am. Ceram. Soc., 1–8 (2013)
DOI: 10.1111/jace.12682

journal

The Effect of Electric Field on Sintering and Electrical Conductivity of Titania

Shikhar K. Jha and Rishi Raj†

Department of Mechanical Engineering, University of Colorado at Boulder, Boulder, Colorado 80309-0427

The effect of DC electric field on sintering, and on the electrical conductivity of undoped rutile, TiO_2 (99.99%), has been investigated at fields ranging from 0 V to 1000 V/cm. The experiments were carried out at a constant heating rate of 10°C/min with the furnace temperatures reaching up to 1150°C. The sintering behavior falls into two regimes: at lower fields, up to 150 V/cm, sintering is enhanced, but densification occurs gradually with time (Type A or FAST sintering). At higher fields sintering occurs abruptly, and is accompanied by a highly nonlinear increase in conductivity, which has been called flash sintering (Type B or FLASH sintering). Arrhenius plots of conductivity yield an activation energy of 1.6 eV in Type A and 0.6 eV in Type B behavior; the first is explained as ionic and the second as electronic conductivity. The evolution of grain size under both types of sintering behavior are reported. These results highlight that the dominant mechanism of field-assisted sintering can change with the field strength and temperature. We are in the very early stages of identifying these mechanisms and mapping them in the field, frequency, and temperature space.

I. Introduction

TiO_2, in its two commonly known forms, anatase, and rutile, have shown promise for applications such as dye-sensitized solar cells[1,2] sensors,[3] and capacitors.[4,5] In another work, the effect of rapid cooling and annealing temperature on the transition from ionic to electronic conductivity in undoped TiO_2 has been reported.[6] Quenching TiO_2 sample from a gradually increasing dwell temperature changes the nature of conductivity from insulator to semiconductor, which has been attributed to freezing of oxygen vacancies in the structure. The effect of atmosphere (with different partial pressure of oxygen) on the conductivity of sample at room temperature has also been evaluated.[6] Doping with pentavalent oxides, such as V_2O_5, Nb_2O_5 which act as donors, raises the dielectric constant, the breakdown strength and the exponent of nonlinearity for the *I–V* plot in varistor applications.[7]

The above properties depend on the sintering treatment, which determines the grain size and the defect concentration. While large grained TiO_2 shows higher electrical conductivity, fine grain structures have been reported to have the highest breakdown strength. Getting a fine grain size is not an easy task because the grain size increases rapidly above ~1000°C.[4] Thus, long hours of sintering at 800°C are needed to avoid grain growth, and even then full densification may not be realized. Two-step sintering methods[8,9] have achieved fine grain sizes with little grain growth, but at the expense of long hold time. Pure titania has been reported to sinter to full density at 1000°C for 20 h.[10] At a constant heating rate of 10°C/min the temperature needs to reach 1150°C to achieve full densification (present work). Doping with aliovalent oxides have shown to enhance sintering, but they promote grain growth as well.[7]

Recently, field-assisted sintering, where the electric field is applied directly to the specimen with a pair of electrodes, has been reported. In the earliest work, the sintering furnace temperature for 3YSZ[11] was reduced from 1400°C to 850°C in constant heating rate experiments with the field of 120 V/cm. In these experiments sintering was accompanied by an abrupt increase in the conductivity of the specimen. Sintering occurred in a few seconds, as if in a flash, which led to it being called flash sintering. Initially, this phenomenon was ascribed to Joule heating,[11] but in a later Raj *et al.*[12] have considered defect avalanche as another possible explanation of this unusual behavior. Baraki *et al.*[13] have reported careful measurements of the specimen temperature in the flash state (by the measurement of thermal expansion), which suggest that Joule heating is not high enough to yield temperatures that can produce sintering in a few seconds [see Appendix]. They have also proposed the effect of flash on grain growth.[13]

Flash sintering as a technique has found applications in different fields such as SOFC[14–16] and tape casting.[16] Application of AC instead of DC fields on field-assisted sintering behavior remains an open question.[17] In the experiments with yttria-doped zirconia, Muccillo *et al.*[18,19] and M'Peko[20] have reported an increase in the grain-boundary conductivity in specimens prepared by flash sintering.

With this background, we attempt to understand the effect of the electric field on the sintering behavior and the electrical conductivity of TiO_2. The influence of the sintering protocol on grain size is studied.

II. Experimental Methods

(1) Materials, Specimens and Sintering Procedure

Rutile nanopowders of purity 99.995% (NP-TiO_2-R-20 MTI Corporation Material Ltd. USA, Richmond, CA) with initial particle size of 20 nm were uniaxially pressed into dog bone–shaped specimens under the load 130 MPa yielding a relative density of ~47.2%. The gage section had a length of 20 mm and a rectangular cross section of 3.4 mm × 1.5 mm. Sample were presintered at 5°C/min to 550°C and held at that temperature for 60 min to remove the binder (5 wt% polyvinyl alcohol).

The specimen was suspended into a vertical tube furnace with a pair of platinum wires, which also served as the electrodes for applying the electric field across the gage section. A DC field was applied to the specimen, and the furnace was heated to 1150°C at a constant heating rate of 10°C/min.

(2) Microstructure Characterization

Sintered samples were cut and polished to 1 μm diamond abrasive and then thermally etched. Grain size measured from fracture surfaces was the same as from the etched and thermally etched specimens. The grain size was determined from micrographs under field emission scanning electron

I.-W. Chen—contributing editor

Manuscript No. 32919. Received March 20, 2013; approved September 27, 2013.
†Author to whom correspondence should be addressed. e-mail: rishi.raj@colorado.edu

microscope (JSM-7401F JEOL, Tokyo, Japan). Grain sizes were then analyzed using linear intercept method with MATLAB. This program also provides a tool to analyze the histogram distribution of grain size.

(3) Measurement of Sintering

A CCD camera, placed underneath the furnace, recorded the shrinkage in the sample as it sintered. The true linear shrinkage strain was calculated using the equation:

$$\varepsilon = \ln(l/l_0) \tag{1}$$

where l_0 is the initial gage length and l is instantaneous gage length. Final density, ρ, is calculated from the linear shrinkage using the following equation[21]:

$$\rho = \rho_g e^{-3\varepsilon} \tag{2}$$

where ρ_g is the normalized green density. Note that as $l < l_0$, the strain, ε, has a negative value. Therefore, in Eq. (2), $\rho > \rho_g$.

The green densities of the samples varied from 0.468 to 0.476, and were assumed to be 0.472. Density was also measured physically by cutting the sintered rectangular gage sections of known volume (length × width × thickness) from the sintered samples and measuring their weights. In addition, the density was measured by the Archimedes method and compared with the geometrical method just described. In a third method the final density, as given by Eq. (2), was estimated from the measurement of the sintering strain. These three estimates of the final density are compared in the results.

(4) Measurement of Conductivity

The phenomenon of flash sintering is characterized by a highly nonlinear rise in electrical conductivity. Under voltage control this effect produces a sudden rise in power dissipation which is limited experimentally by switching the power supply from voltage to current control (the switching time is specified to be 10 ms). Under current control the sample stabilizes to a steady-state voltage, determined by the intrinsic conductivity of the specimen in the flash state. The conductivity in this activated state was obtained by dividing the current density by the electric field.

The baseline data for the temperature-dependent conductivity of TiO_2 was obtained from the four-probe method on conventionally sintered titania. A field of 5 V/cm was used for these measurements. These specimens had a grain size of ~1.7 μm.

(5) The Measurement of Temperature

The nature of field-assisted sintering falls (at least) into two regimes:

1. The low-field regime where the conductivity of the specimen continues to follow the nominal Arrhenius behavior determined by ionic diffusion. In this regime sintering is somewhat enhanced by Joule heating, but the effect is minor and does not spell a change in the mechanism of conductivity.[20] We call this Type A or FAST sintering behavior.
2. The high-field regime where "flash sintering" is accompanied by a highly nonlinear increase in the conductivity of the specimen. We call this Type B for FLASH sintering behavior. The nonlinear rise is conductivity is limited experimentally by switching the power supply from voltage to current control. Under current control, the specimen settles to a steady-state power input into the specimen. In this state, the temperature of the specimen is measured directly with a pyrometer. The specimen temperature is also estimated from a blackbody radiation model[11,21,22] where the power dissipation is equated to increased radiation (which scales as the fourth power of the temperature) to determine the steady-state temperature. As other losses such as convection and conduction are neglected, the model gives an upper bound for the temperature. According to this model the specimen temperature, T^*, is related to the furnace temperature, T_0, by the following equation[21]:

$$\frac{T^*}{T_0} = \left[1 + \frac{1000 W_V}{\sigma T_0^4}\left(\frac{V}{A}\right)\right]^{\frac{1}{4}} \tag{3}$$

where the temperatures are expressed in K. The power dissipation per unit volume of the specimen is given by W_V, in units of mW/mm^3. The volume to surface area of the specimen is (V/A) written in units of mm (for our samples it value is equal to 0.5 mm). σ is blackbody radiation constant, being equal to 5.67×10^{-8} $Wm^{-2}K^{-4}$. The equation assumes the emissivity to be equal to unity. It is usually ~0.9 for oxides which would raise the specimen temperature somewhat above that predicted by Eq. (3). The validity of Eq. (3) had been established against experimental data where the temperature of specimens in the flash state was measured exactly through thermal expansion for various levels of power dissipation.[13] Further discussion of Joule heating of the specimens is given after presenting results from this work. It is further discussed in the Appendix.

III. Results

(1) Sintering Behavior at Low and High Fields

The linear shrinkage strain plots with applied field ranging from 0 V (conventional sintering) to 1000 V/cm are shown in Fig. 1. For fields of less than 50 V/cm the shrinkage coincides with conventional sintering data (0 V). At fields of up to 150 V/cm sintering rate is enhanced, but the character of the sintering curves continues to behave as in conventional sintering, that is, sintering occurs gradually with time. At higher fields sintering occurs abruptly, in mere seconds, which we have called flash sintering. The behavior at low fields is classified at Type A behavior, whereas flash sintering at the higher fields is being called Type B behavior. The transition from the Type A to Type B behavior is gradual. For example, at 150 V/cm sintering appears to be a combination of A and B, with the abrupt increase in sintering taking place

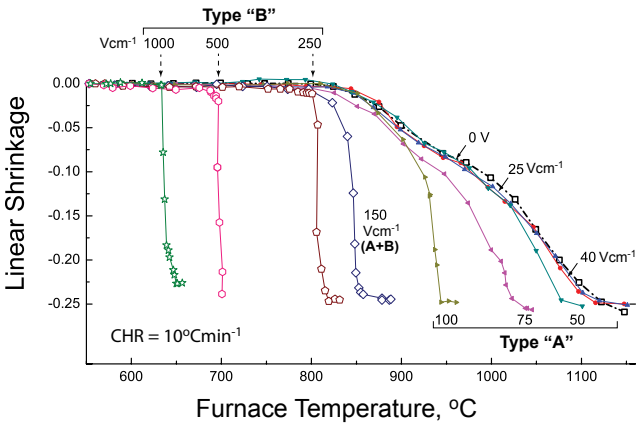

Fig. 1. Sintering curves for the linear shrinkage measured at different applied DC fields in experiments carried out at constant heating rate.

after a shrinkage of about 0.12. In the following section, we describe a formal procedure for separating the sintering strain into Type A and Type B.

The procedure recognizes that the TiO_2 specimens exhibit a nonlinear rise in electrical conductivity at a threshold temperature in a constant heating rate experiment. This phenomenon is shown by the results in Fig. 2, where a nonlinear increase in conductivity is seen at fields of 50 V/cm or greater. These data show two important features of the experiments: (i) the rise in power dissipation is limited by switching the power supply from voltage to current control, which leads to a decline in power dissipation toward a steady state, and (ii) the nonlinear increase is conductivity is not necessarily coupled to sintering: in Type A behavior sintering occurs before the onset of the nonlinearity, whereas in Type B behavior the nonlinearity and sintering occur together in what has been called flash sintering.

Point (ii) above is explained by the data in Fig. 3 where the shrinkage data and the electrical behavior are plotted synchronously. Two situations, one at an applied field of 100 V/cm, and the other at 500 V/cm are shown. The electrical nonlinearity occurs at ~935°C at the low field and at ~700°C at the higher field. The shrinkage strain is given by the *y*-axis on the left: at high field all the shrinkage strain occurs in the flash state, but at the lower field one-half of the densification strain has occurred before the onset of the flash. This procedure was repeated at different fields to separate the densification into Type A (before flash) and Type B (after flash) regimes. The results of this exercise are given in Fig. 4, which shows that the mechanism of field-assisted sintering changes from one to the other as the field is increased.

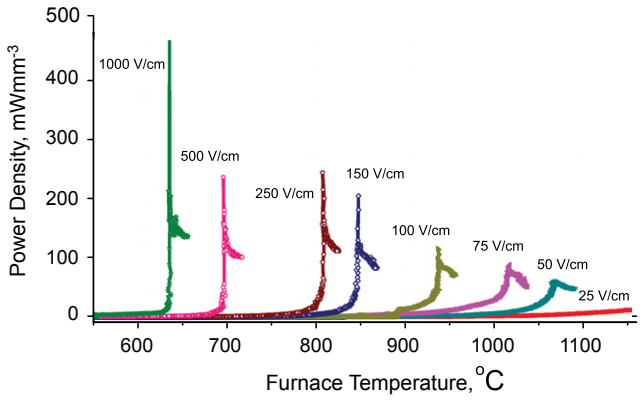

Fig. 2. Power dissipation plots near the "flash" temperature for various DC fields.

(2) Density as a Function of the Electric Field

The final density of the specimens, estimated by the three methods (strain, Archimedes, and physical), are given in Fig. 5. The density calculated from the shrinkage is consistently somewhat higher than from the other two methods. Most likely this can be attributed to slight differences in the shrinkage in the thickness and width directions than in the longitudinal direction because of anisotropic packing of particles as the green samples were prepared by uniaxial pressing.

(3) Electrical Conductivity

The baseline values for the electrical conductivity of dense TiO_2 made by conventional sintering was measured by the four-probe technique under a field of 5 V/cm at temperatures up to 1200°C. The results are shown by the solid black line in Fig. 6. As was expected the behavior is Arrhenius with an activation energy of 1.6 eV, which is in good agreement with literature values.[23]

The conductivities from the flash experiments at different levels of electrical fields are given in various colors in Fig. 6. Note that while the conductivities are below the conductivity of the dense specimen (described above), most likely due to the porous nature of the specimens, they rise precipitously at the onset of the nonlinearity.

The conductivity measurements, therefore, show two regimes of behavior. Before the flash, the conductivities are in reasonable agreement with the ionic conductivity of dense specimens, but after the flash the conductivities are much higher. It was possible to calculate the conductivities in the flash regime because under current control the specimens relax to a steady state as seen by the plateaus just after the peaks in Fig. 2. The conductivities obtained in this manner just after the flash temperature are plotted in Fig. 7, which also contains the data from the four-probe measurements of fully sintered specimens at 5 V/cm. The activation energy for the "flash state" is 0.59 eV far below the activation energy for ionic diffusion. Note that the temperatures given in Fig. 7 for the flash-state refer to the specimen temperatures as estimated from the blackbody radiation model. This point is discussed in the following section.

(4) Joule Heating

In the flash regime, the specimens operate under current control and develop a steady-state voltage as determined by the conductivity in this activated state. This phenomenon is explained in Fig. 8, where the power input into the specimen is plotted against the specimen temperature. The current supplied to the specimen is held constant; therefore, if the specimen temperature were to rise the power dissipated within it

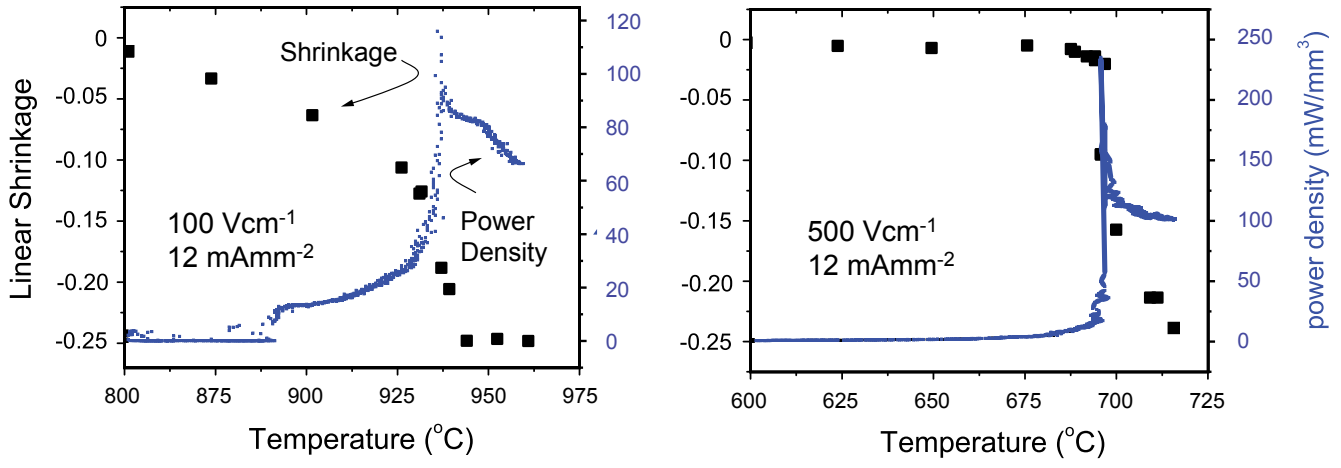

Fig. 3. The synchronization between sintering and the nonlinear increase in conductivity (the flash event) at two different applied fields.

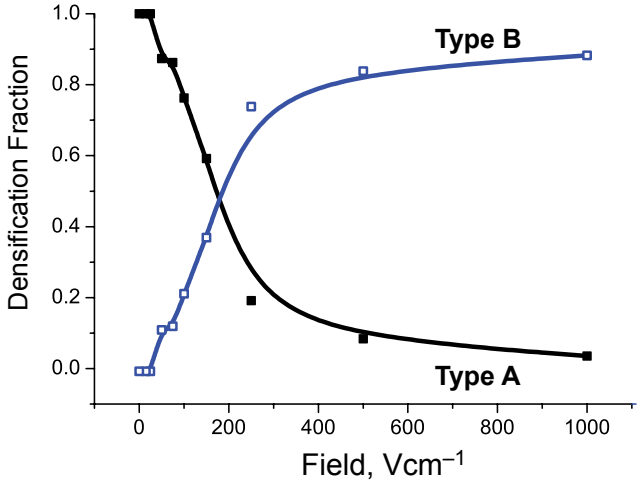

Fig. 4. Partitioning of densification strain attributed to Type A and Type B behaviors.

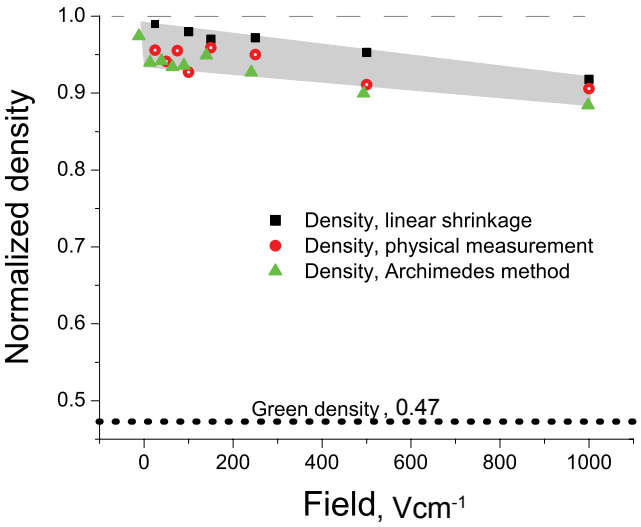

Fig. 5. The density of the sintered specimens as a function of the applied field under which they were sintered.

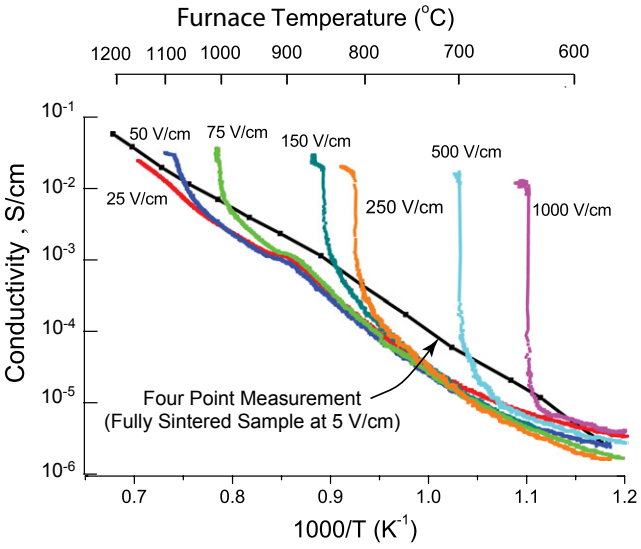

Fig. 6. The change in the conductivity of the specimens as they sinter. The abrupt increase in the conductivity is a signature of the flash event. The black line gives the baseline ionic conductivity of conventionally sintered specimens.

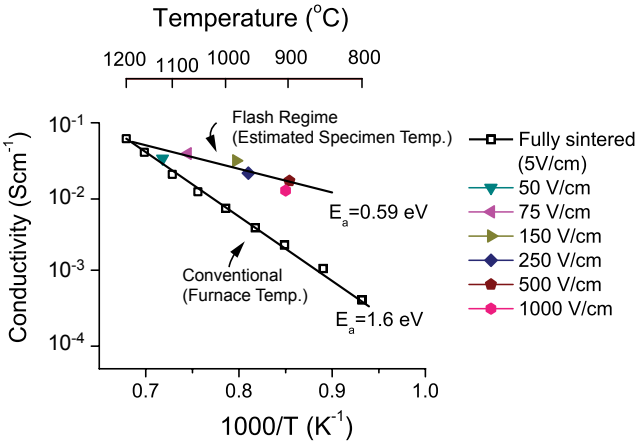

Fig. 7. An Arrhenius plot of the conductivity of the specimen in the flash regime. It gives a much lower activation energy than the conductivity measured for a dense specimen at weak fields, where the conduction is predominantly ionic.

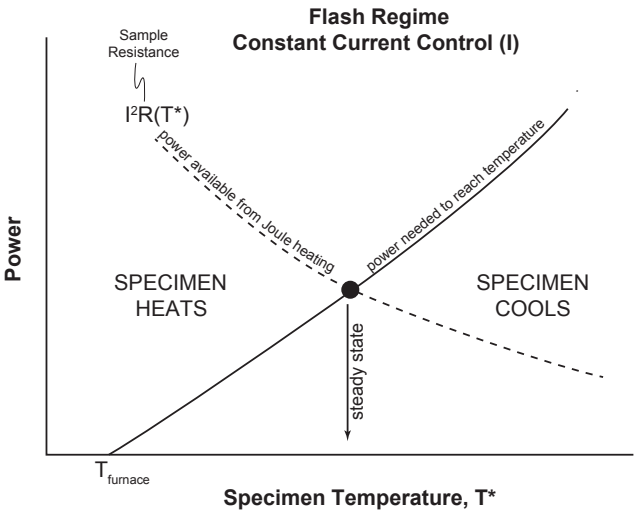

Fig. 8. The specimen reaches a steady-state temperature in the flash regime by finding the balance between its change in resistance, which controls electrical dissipation and blackbody radiation. Both are functions of temperature, but in opposite ways.

would fall. On the other hand the power needed to raise the specimen temperature increases with temperature because blackbody radiation increases with the fourth power of temperature. Thus, an equilibrium is established where the power dissipation required to maintain the specimen temperature is equal to what the current can supply. The specimen heats if it is below, and cools if it is above this temperature.

These results that give the furnace temperature, the specimen temperature, and the power dissipation are given in Table I. The sample temperature and the furnace temperature are plotted in Fig. 9. The error bars in the former include the uncertainty arising from the fluctuation in the voltage measurement and as well as 0.9–1.0 in the value of the emissivity of the sample. The flash regime occupies the high fields (above ~200 V/cm) where the sample temperature is in the 800°C–950°C range. These temperatures are far below the temperatures that would be required to sinter TiO_2 in just a few seconds (conventional sintering requires ~1100°C for a few hours).

(5) Microstructure

The grain size of all samples sintered under the electric field was measured. Micrographs for three cases along with the grain size distributions are shown in Fig. 10, and the values

Table I. Listing of Experimental Parameters, and from them the Derivation of the Specimen Conductivity and Estimated Temperature of Sample in the Flash (Type B) Regime

Applied field, Pre-flash, (V/cm) (under voltage control)	Post flash field, (V/cm) (under current control)	Current density during flash (mA/mm^2)	Conductance (S/cm)	Power density (mW/mm^3)	Furnace temperature (°C)	Sample temperature (°C)
0	n/a (voltage control)	0	0.027	0	1150	1150
15		2.4	0.027	3.6	1150	1152 ± 1
25		5	0.019	10	1150	1158 ± 2
40		9.7	0.026	39	1150	1178 ± 7
50	47	12 (current control)	0.033	52	1077	1121 ± 10
75	45		0.026	60	1000	1060 ± 12
100	59		0.019	75	930	1015 ± 18
150	60		0.021	95	840	968 ± 24
250	87		0.015	118	780	984 ± 33
500	100		0.012	110	700	896 ± 35
1000	105		0.011	149	640	917 ± 44

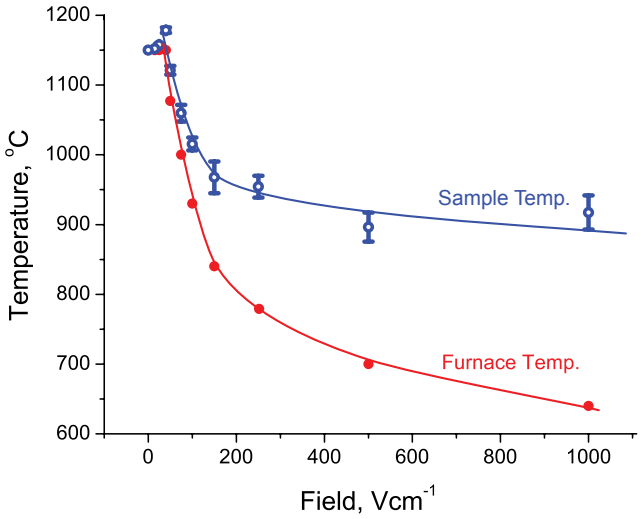

Fig. 9. The divergence between the furnace and the specimen temperature. The full data, including the power dissipation are given in Table I.

from all experiments are plotted in Fig. 11. The grain size clearly decreases in Type A sintering and increases slightly or remains unchanged in Type B behavior. Curiously at small fields (less that 40 V/cm), there is a rapid increase in the grain size with the applied field. While the reason for this behavior is not clear, it explains why these low fields do not show enhanced sintering (Fig. 1): we speculate that the increase in grain size overrides the benefit of the electric field to the sintering rate when the fields are small.

The grain microstructure in the flash sintered samples was isotropic and equiaxed, even though the experiments were carried out under a DC field. Furthermore, we were unable to identify any differences in the grain size and the density across the gage section of the specimens; this was probably because the specimen geometry had been designed to achieve a uniform current density through the gage section, assured by placing the electrode contacts at the large handles of the dog bone–shaped specimens.

IV. Discussion

(1) Mechanisms of Field-assisted Sintering and Conductivity

The influence of electrical fields on mass transport and electrical conductivity in ceramics, particularly the oxides, can have various outcomes, depending on the temperature and the electrical control parameters. Just as the dominant mechanisms underlying the mechanical response of materials can change with temperature, the applied stress, the microstructure, and the duration of the test, so can the response of ceramics to applied fields vary with temperature, the strength of the electrical field and the time-dependent shape of the power cycle and the microstructure (for example the effect of particle size[24]). In mechanical experiments, one can control either the applied stress or the strain rate, not both, so it is in the present experiments where it is possible to control either the voltage or the current.

The results presented here show that at least two different mechanisms in field-assisted sintering can operate. At low fields (Type A), sintering is enhanced but without a nonlinear increase in the electrical conductivity, whereas at high fields sintering occurs as if in a flash (Type B) with the effect being invariably accompanied by a highly nonlinear increase in electrical current. The power dissipation in the sample is given by the voltage times the current; thus the ever increasing current can lead to unbounded Joule heating of the specimen. Control is exercised by limiting the current flowing through the specimen after the onset of the flash. The specimen then finds its own electrical steady state in temperature and conductivity, dictated by a balance between blackbody radiation and the change in conductivity with temperature (Fig. 8). The design of the electrical parameters at the power supply has been germane to obtaining a well-controlled and reproducible effect of sintering in the flash regime. It is important to recognize that different mechanisms of field-assisted sintering and electrical conductivity can be invoked by changing the strength of the electrical field, the current limit, and the temperature.

(2) The Experimental Space: AC/DC Power, Voltage and Current Control, and Joule Heating

Preliminary results from our laboratory with AC fields are revealing that in addition to the voltage and current, the frequency of the electrical fields can influence the outcome of the experiment. The magnitude of the electric field, the current setting, the frequency, and the temperature can lead to different results, reflecting different mechanisms for field-assisted sintering. This point is often overlooked leading to unnecessary controversy when comparing results from different laboratories.

The role of Joule heating in flash sintering is an example of such a controversy. Surely, a sample left under voltage control in the flash regime would continue to heat up, become unstable, and eventually melt [see Appendix]. Recent results from Park and Chen[25] where they estimate the sample to reach a temperature of 2500°C under voltage control is an

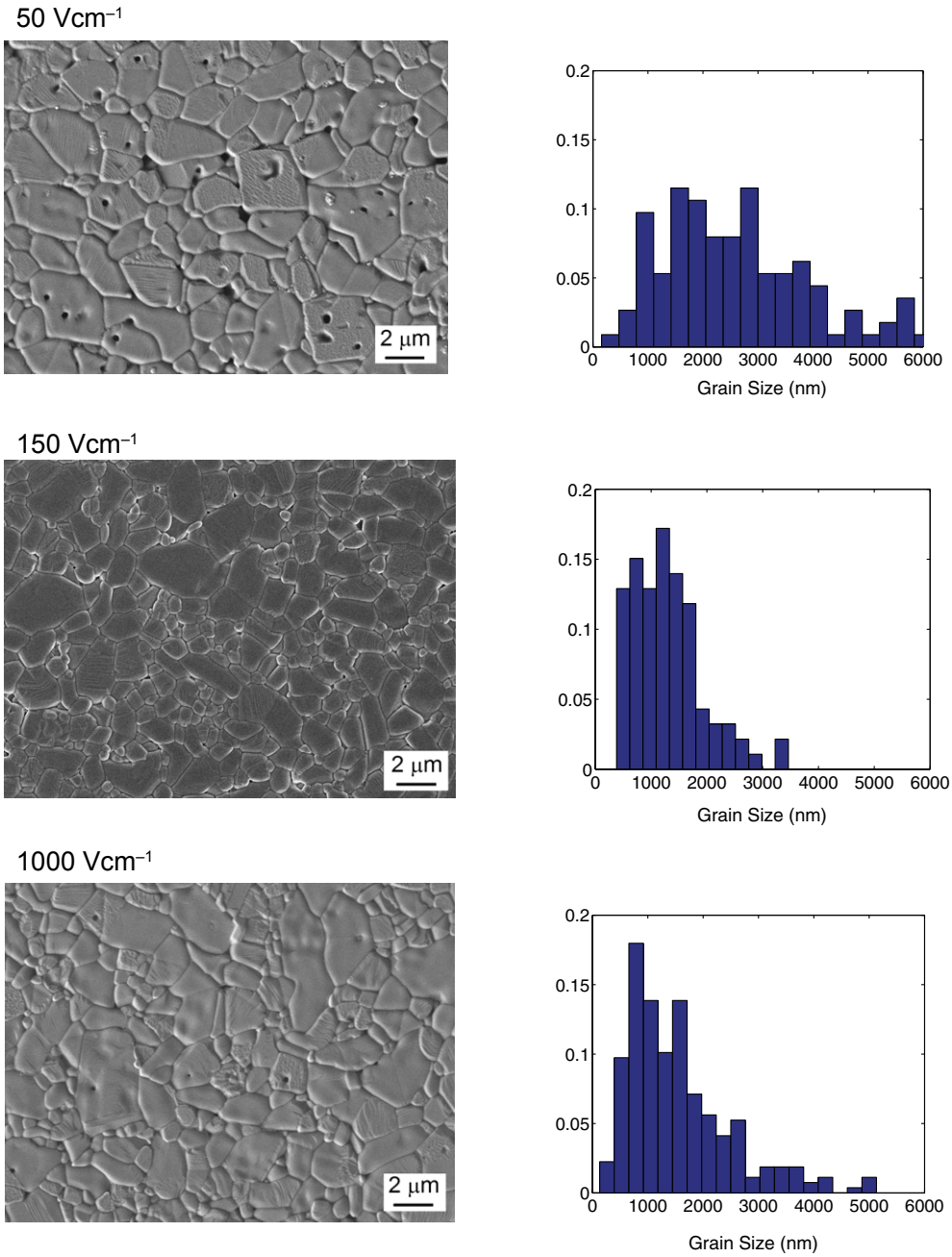

Fig. 10. SEM micrographs of specimens showing the grain microstructure of specimens sintered under different applied fields. The distribution of the grain size is included on the right.

example of this disconnect with the current controlled experiments conducted in our laboratory. The 300 kHz fields used by Park and Chen[25] stand in contrast to the DC fields in our experiments which throw further uncertainty into this comparison. Furthermore, we are also dubious about the method used by Park and Chen to estimate the sample temperature: they extrapolate the low-field Arrhenius ionic conductivity data obtained up to ~1400°C, to 2500°C (well beyond 1400°C), which lies in the flash regime where the mechanism of conductivity changes. The results in Fig. 7 show that the activation energy for conductivities in the flash regime is very different from the low-field ionic regime, which raises doubt about the Park and Chen[25] approach for estimating the sample temperature.

Recently, Steil *et al.*[26] have reported systematic experiments on the effect of current density after the initiation of the flash on densification behavior of 8 mol% YSZ. Their finding that the density increases with the current setting is in agreement with the work from this laboratory.[27] However, their final densities are somewhat lower, even though the steady-state power levels achieved in current control were higher than our experiments. It is possible that this difference reflects the use of 1000 Hz AC electrical fields as opposed to the DC fields. They also estimate an upper bound value for the specimen temperature of 1710°C based upon adiabatic heating during the power spike which occurs when switching from voltage to current control. Blackbody radiation loss, which rises as the fourth power of the temperature and occurs instantaneously, will reduce the temperature to well below 1710°C. Nevertheless, it still does not explain the sintering of YSZ in one or two-seconds since it is estimated that the specimen would have to be at 1910°C to sinter in a few seconds.[22]

To our knowledge, the only direct estimates of the specimen temperature in the flash regime are from the measurement of thermal expansion,[13] and the measurements with two different pyrometers in this laboratory. These estimates are self-consistent and in good agreement with predictions

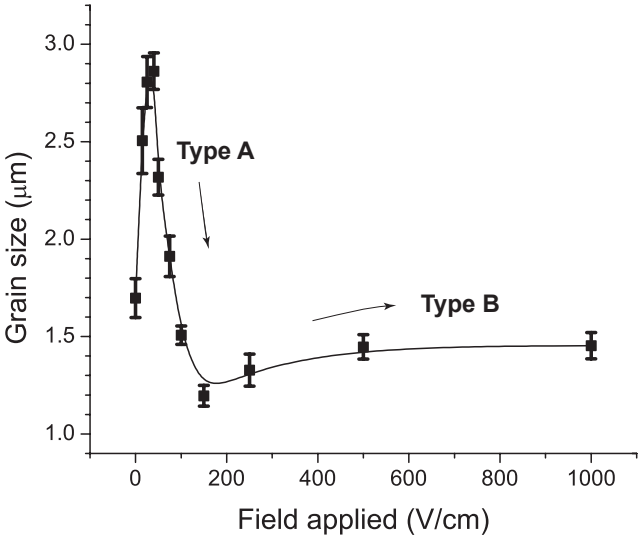

Fig. 11. Measurements of the grain size in the specimens sintered at different applied fields. A decline in the grain size under Type A and a small increase under Type B sintering are consistent with earlier work on yttria-stabilized zirconia, but grain growth at very low fields for the present experiments on titania has not be seen before.

from a blackbody radiation model. Collectively, these results show that flash sintering occurs at temperatures that are well below the temperature that would be required to sinter YSZ in just a few seconds.

The specimen geometry also plays in these experiments. We use dog-cone specimens hung into the furnace with platinum wires hooked through holes in the handles of these specimens. Platinum paste is used to spread the current flowing into the specimen. The dog-bone shape assures that the current flow is uniform through the narrower cross section of the gage length. Uniformity of the grain size across the gage length confirms this effect.

(3) Grain Growth under Electric Field

Type A behavior, which was first reported in the sintering of 3 mol% yttria-stabilized zirconia at low fields,[11] was explained by the reduced rate of grain growth under weak electrical fields. As sintering rate increases (inversely) with the fourth power of the grain size, even a modest reduction in grain size can produce a significant increase in the rate of sintering. The convergence between the reduced rate of grain growth and higher rates of sintering has successfully explained Type A behavior in yttria-stabilized zirconia.[21,28]

As in YSZ, we find that grain growth is retarded in the low-field regime, marked as Type A behavior in Fig. 11, for fields ranging from 40 to 150 V/cm. However, the results given by the two points to the left, showing an increase in the grain size with the field are anomalous. These experiments were repeated to ascertain their reproducibility. We do not have a reasonable explanation of these two points.

The results for Type B regime stand in contrast to Type A behavior: we find that in the flash regime, the grain size exhibits a tendency to increase, which is opposite to the low-field behavior.

The spectrum of results in Fig. 11 illustrates the complex influence of electric fields on the grain size. The results in Ghosh *et al.*[28] have shown that weak electrical fields applied to fully sintered polycrystals of zirconia can retard grain growth. The explanations for the reduced rate of grain growth under electric fields have centered on a change in the interfacial energy with applied field, either because of some degree of local heating at grain boundaries, which lowers the energy due to the entropy,[23] or due to an interaction between electric field and the space charge at the boundaries.[29] The influence of electrical fields on grain growth in the Type B regime is variable and remains unpredictable at the present time.

V. Summary

1. The electrical control parameters, along with the temperature, can be varied to induce different mechanisms of sintering and electrical conductivity. At low fields, the conductivity remains Arrhenius having the activation energy for ionic diffusion and the sintering rate is modestly enhanced (Type A). At high fields, conductivity rises highly nonlinearly and the power supply must be switched to current control to obtain stable behavior. In this regime, the conductivity is most likely electronic with lower activation energy than for ionic diffusion. Most remarkably, in the Type B regime sintering occurs in just a few seconds.
2. Just as mechanical response of materials can be dominated by different mechanisms that come into play at different levels of applied stress (or strain rate), temperature and microstructure, so can the effect of electrical driving forces lead to various mechanisms of mass and charge transport that depend on the strength of the field, the current, the frequency, and the microstructure.
3. The evolution of the grain size displayed by the results in Fig. 11, further demonstrates changes in the dominant atomistic mechanism as a function of the strength of the electrical field. The increase in grain size at very low fields, though reproducible, is anomalous, and remains unexplained. The grain size decreases with field in the Type A regime, but then increases slightly in Type B regime.
4. In the present experiments, the extent of Joule heating was limited by switching the power supply to current control, which leads to a quasi-steady state of electrical conduction. Measurements of specimen temperature in this state, as well as the predictions from a blackbody radiation model yield specimen temperatures that are well below that required for sintering in just a few seconds.
5. For our phenomenological knowledge to progress into atomistic understanding, it is necessary to recognize that more than one mechanism can prevail in field-assisted sintering. The experiments suggest unusual couplings between mass transport, nonlinear changes in electrical conductivity, and the evolution of the grain size.

Appendix

The extensive review of this manuscript reveals a deep-seated controversy about the mechanism of flash sintering. A highly nonlinear rise in conductivity is a signature of this event, which leads us to the rather simple perception that the sample is suffering a very high level of Joule heating, enough to account for sintering in mere seconds. Indeed, that was our impression as well in the first paper published in November 2010.[11] There are at least a few points that can be made on this issue.

It is becoming increasingly clear that electric fields and currents can influence response of a ceramic material in different ways. What may apply at very high current densities may not be true at low currents. Claims are made in the literature, for example in Ref. [30], that samples show melting behavior; however, in this study there is no information about the current densities used in the experiment. Certainly, if the current is allowed to rise in an uncontrolled way then I^2R heating will eventually lead to melting. Care is needed when comparing results from different experiments. Just as deformation mechanism maps caution us to recognize that

the material response depends on temperature and stress, so does the electrical response of a material depend upon the field, the current, and the temperature. It is critical to state the current density, the field, and the temperature when describing the material response. Extrapolations from one mechanism regime into a different regime can lead to incorrect conclusions.[30]

Two papers have discussed the influence of electric field and current on the temperature of the specimen. They are Baraki *et al.*[13] and Raj.[22] Please note that the Raj paper builds on the Baraki *et al.* paper. When reading these papers please recognize that there are the two regimes of power dissipation. The experiments begin by applying a constant voltage to the specimen, which at a threshold value of the temperature produces a highly nonlinear increase in the conductivity (for reasons that we do not understand). In this regime, Regime I, the power dissipation is given by V^2/R; as the resistance falls the power dissipation rises. When the current reaches a preset limit the power supply switches to current control, which happens in 10 ms according to specifications. This is the second regime, Regime II, where the power dissipation is now given by I^2R; the power dissipation now declines as the resistance continues to fall, and quickly reaches a steady state.

Baraki *et al.*[13] give the relationship between the specimen temperature and power dissipation in Regime II. These measurements are in good agreement with predictions from a blackbody radiation model.[22] These measurements and comparison with the model have been confirmed many times in different experiments in our laboratory. Typically they produce an increase in specimen temperature in the range 100°C–400°C for a power dissipation of about 100–400 mW/mm^3.

Baraki *et al.*[13] also show the presence of a sharp peak in power dissipation (Regime I) which precedes the steady state (Regime II). However, they do not find a corresponding spike in specimen temperature. This issue is has been carefully and quantitatively analyzed[22] in terms of the heat content required to raise the specimen temperature to the steady-state levels, as required by the specific heat of the material. It is concluded that in Regime I, the spike in power dissipation is damped by the specific heat of the specimen. Measurements of the specimen temperature with a pyrometer in our laboratory are consistent with this expectation: they do not show a spike in the specimen temperature corresponding to the spike in the power dissipation.

Suggestions have been made that the specimen interior can heat to very high levels while the surface remains at a lower temperature. Again, this would depend on the mechanism by which the specimen responds to the applied field and current. In the work reported from our laboratory, we have limited our experiments to situations where there is no localization of current in the specimen. The design of the specimens, the dog-bone shape, assures a uniform flow of current through the gage section. Microstructural analyses do not exhibit a gradient from the surface toward the interior. If the power dissipation in the specimen is uniform there is no convincing reason (from the point of view of heat transfer) to expect a large temperature gradient within the specimen as most of the heat loss is from blackbody radiation.

However, as stated above, there are different regimes of behavior depending on the field and the current. We have evidence that at very high current settings at the power supply, the current through the specimen can localize causing "tunneling" to some degree. However, these current levels spell a different regime of behavior, and we shall be reporting on this in the near future.

Acknowledgment

This research was supported by the Basic Science Division of the Department of Energy under grant no: DE-FG02-07ER46403. We thank Dr. John S. C. Francis for his continuous help and advice.

References

[1]H. C. Weerasinghe, P. M. Sirimanne, G. V. Franks, G. P. Simon, and Y. B. Cheng, "Low Temperature Chemically Sintered Nano-Crystalline TiO_2 Electrodes for Flexible Dye-Sensitized Solar Cells," *J. Photochem. Photobiol., A*, **213** [1] 30–6 (2010).

[2]N.-G. Park, K. M. Kim, M. G. Kang, K. S. Ryu, S. H. Chang, and Y.-J. Shin, "Chemical Sintering of Nanoparticles: A Methodology for Low-Temperature Fabrication of Dye-Sensitized TiO_2 Films.," *Adv. Mater.*, **17** [19] 2349–53 (2005).

[3]T. Bak, J. Nowotny, M. K. Nowotny, and l. R. Sheppard, "Defect Engineering of Titanium Dioxide," *J. Aust. Ceram. Soc.*, **44** [2] 63–7 (2008).

[4]S. Chao, V. Petrovsky, and F. Dogan, "Effects of Sintering Temperature on the Microstructure and Dielectric Properties of Titanium Dioxide Ceramics," *J. Mater. Sci.*, **45** [24] 6685–93 (2010).

[5]M. Radecka, "Effect of High-Temperature Treatment on n — P Transition in Titania," *J. Am. Ceram. Soc.*, **85** [2] 346–54 (2002).

[6]Y. Liu and A. R. West, "Semiconductor-Insulator Transition in Undoped Rutile, TiO_2, Ceramics," *J. Am. Ceram. Soc.*, **96** [1] 218–22 (2013).

[7]M. Zou, Y. Wang, y. Chen, and Y. Zhang, "Influence of Donar Additives and Properties of TiO_2-Based Varistor.," *Adv. Mater. Res.*, **105**, 320–3 (2010).

[8]I. Chen and X. Wang, "Sintering Dense Nanocrystalline Ceramics Without Final-Stage Grain Growth.," *Nature*, **404** [6774] 168–71 (2000).

[9]M. Mazaheri, A. Zahedi, M. Haghighatzadeh, and S. K. Sadrnezhaad, "Sintering of Titania Nanoceramic: Densification and Grain Growth.," *Ceram. Int.*, **35** [2] 685–91 (2009).

[10]H. Hahn, J. Logas, and R. S. Averback, "Sintering Characteristics of Nanocrystalline TiO_2," *J. Mater. Res.*, **5** [3] 609–14 (1990).

[11]M. Cologna, B. Rashkova, and R. Raj, "Flash Sintering of Nanograin Zirconia in <5 s at 850°C," *J. Am. Ceram. Soc.*, **93** [11] 3556–9 (2010).

[12]R. Raj, M. Cologna, and J. S. C. Francis, "Influence of Externally Imposed and Internally Generated Electrical Fields on Grain Growth, Diffusional Creep, Sintering and Related Phenomena in Ceramics," *J. Am. Ceram. Soc.*, **94** [7] 1941–65 (2011).

[13]R. Baraki, S. Schwarz, and O. Guillon, "Effect of Electrical Field/Current on Sintering of Fully Stabilized Zirconia," *J. Am. Ceram. Soc.*, **95** [1] 75–8 (2012).

[14]M. Cologna, A. L. G. Prette, and R. Raj, "Flash-Sintering of Cubic Yttria-Stabilized Zirconia at 750°C for Possible Use in SOFC Manufacturing," *J. Am. Ceram. Soc.*, **94** [2] 316–9 (2011).

[15]Y. Liu, X. Hao, Z. Wang, J. Wang, J. Qiao, Y. Yan, and K. Sun, "A Newly-Developed Effective Direct Current Assisted Sintering Technique for Electrolyte Film Densification of Anode-Supported Solid Oxide Fuel Cells," *J. Power Sources*, **215**, 296–300 (2012).

[16]M. Cologna, V. M. Sglavo, and M. Bertoldi, "Sintering and Deformation of Solid Oxide Fuel Cells Produced by Sequential Tape Casting," *Int. J. Appl. Ceram. Technol.*, **7** [6] 803–13 (2010).

[17]R. Muccillo, M. Kleitz, and E. N. S. Muccillo, "Flash Grain Welding in Yttria Stabilized Zirconia," *J. Eur. Ceram. Soc.*, **31** [8] 1517–21 (2011).

[18]R. Muccillo, E. N. S. Muccillo, and M. Kleitz, "Densification and Enhancement of the Grain Boundary Conductivity of Gadolinium-Doped Barium Cerate by Ultra Fast Flash Grain Welding," *J. Eur. Ceram. Soc.*, **32** [10] 2311–6 (2012).

[19]R. Muccillo and E. N. S. Muccillo, "An Experimental Setup for Shrinkage Evaluation During Electric Field-Assisted Flash Sintering: Application to Yttria-Stabilized Zirconia," *J. Eur. Ceram. Soc.*, **33** [3] 515–20 (2013).

[20]J.-C. M'Peko, J. S. C. Francis, and R. Raj, "Impedance Spectroscopy and Dielectric Properties of Flash Versus Conventionally Sintered Yittria Doped Zirconia Electroceramics Viewed at the Microstructural Level," *J. Am. Ceram. Soc.* (2013). under review.

[21]D. Yang, R. Raj, and H. Conrad, "Enhanced Sintering Rate of Zirconia (3Y-TZP) Through the Effect of a Weak dc Electric Field on Grain Growth," *J. Am. Ceram. Soc.*, **93** [10] 2935–7 (2010).

[22]R. Raj, "Joule Heating During Flash-Sintering," *J. Eur. Ceram. Soc.*, **32** [10] 2293–301 (2012).

[23]A. L. Linsebigler, G. Lu, and J. T. Yates, "Photocatalysis on TiO_2 Surfaces: Principles, Mechanisms, and Selected Results," *Chem. Rev.*, **95** [3] 735–58 (1995).

[24]J. S. C. Francis, M. Cologna, and R. Raj, "Particle Size Effects in flash Sintering," *J. Eur. Ceram. Soc.*, **32**, 3129–36 (2012).

[25]J. Park and I.-W. Chen, "In Situ Thermometry Measuring Temperature Flashes Exceeding 1700°C in 8 mol% Y_2O_3 -Stablized Zirconia Under Constant-Voltage Heating," *J. Am. Ceram. Soc.*, **96** [3] 697–700 (2013).

[26]M. C. Steil, D. Marinha, Y. Aman, J. R. C. Gomes, and M. Kleitz, "From Conventional ac Flash-Sintering of YSZ to Hyper-Flash and Double Flash," *J. Eur. Ceram. Soc.*, **33** [11] 2093–101 (2013).

[27]J. S. C. Francis and R. Raj, "Influence of the Field and the Current Limit on Flash Sintering at Isothermal Furnace Temperatures," *J. Am. Ceram. Soc.*, **96** [9] 2754–8 (2013).

[28]S. Ghosh, A. H. Chokshi, P. Lee, and R. Raj, "A Huge Effect of Weak dc Electrical Fields on Grain Growth in Zirconia," *J. Am. Ceram. Soc.*, **92** [8] 1856–9 (2009).

[29]H. Conrad, "Space Charge and Grain Boundary Energy in Zirconia (3Y-TZP)," *J. Am. Ceram. Soc.*, **94** [8] 3641–2 (2011).

[30]J. Narayan, "A new Mechanism for Field-Assisted Processing and Flash Sintering of Materials," *Scripta Mater.*, **69**, 107–11 (2013). □